NAVAL POSTGRADUATE SCHOOL
Monterey, California

THESIS

FREE SURFACE SCARS AND STRIATIONS

by

Douglas Harris Rau

June 1989

Thesis Advisor: T. Sarpkaya

Approved for public release; distribution is unlimited.

Unclassified

Security Classification of this page

REPORT DOCUMENTATION PAGE

1a Report Security Classification: Unclassified		1b Restrictive Markings	
2a Security Classification Authority		3 Distribution Availability of Report: Approved for public release; distribution is unlimited	
2b Declassification/Downgrading Schedule			
4 Performing Organization Report Number(s)		5 Monitoring Organization Report Number(s)	
6a Name of Performing Organization: Naval Postgraduate School	6b Office Symbol (*If Applicable*): 39	7a Name of Monitoring Organization: Naval Postgraduate School	
6c Address (*city, state, and ZIP code*): Monterey, CA 93943-5000		7b Address (*city, state, and ZIP code*): Monterey, CA 93943-5000	
8a Name of Funding/Sponsoring Organization	8b Office Symbol (*If Applicable*)	9 Procurement Instrument Identification Number	
8c Address (*city, state, and ZIP code*)		10 Source of Funding Numbers	
		Program Element Number	Project No / Task No / Work Unit Accession No

11 Title (*Include Security Classification*): Free Surface Scars and Striations

12 Personal Author(s): Douglas Harris Rau

13a Type of Report	13b Time Covered	14 Date of Report (*year, month,day*)	15 Page Count
Master's Thesis	From To	June 1989	59

16 Supplementary Notation: The views expressed in this thesis are those of the author and do not reflect the official policy or position of the Department of Defense or the U.S. Government.

17 Cosati Codes			18 Subject Terms (*continue on reverse if necessary and identify by block number*)
Field	Group	Subgroup	Unsteady Flow, Vortex Dynamics, Scars, Striations, Surface

19 Abstract (*continue on reverse if necessary and identify by block number*)

A numerical and experimental investigation of the interaction of a pair of vortices with a free surface has been undertaken. The analysis is based on the vortex-sheet representation of the free surface and the use of the appropriate boundary conditions. The experiments were performed in a large basin and the vortices were generated through the use of a special nozzle. The rise of the resulting Kelvin oval, the trajectories of the vortices, and the instantaneous shape of the free surface were recorded on a video tape and then carefully analyzed through the use of a Motion Analysis system. The results have shown that the rise of the vortices not only gives rise to two scars, with a pronounced hump in the middle, but also, and more importantly, to a three-dimensional instability heretofore unknown. The measured and calculated vortex trajectories and the free-surface shapes at the corresponding times and Froude numbers are found to be in reasonable agreement. The new instability will form the basis of future investigations.

20 Distribution/Availability of Abstract	21 Abstract Security Classification	
[X] unclassified/unlimited [ ] same as report [ ] DTIC users	Unclassified	
22a Name of Responsible Individual: Professor T. Sarpkaya	22b Telephone (*Include Area code*): (408) 646-3425	22c Office Symbol: 69Si

DD FORM 1473, 84 MAR 83 APR edition may be used until exhausted security classification of this page

All other editions are obsolete Unclassified

Approved for public release; distribution is unlimited

Free Surface Scars and Striations

by

Douglas Harris Rau
Commander, United States Navy
B.S., United States Naval Academy, 1974

Submitted in partial fulfillment of the
requirements for the degree of

MASTER OF SCIENCE IN MECHANICAL ENGINEERING

and

MECHANICAL ENGINEER

from the

NAVAL POSTGRADUATE SCHOOL
June 1989

ABSTRACT

A numerical and experimental investigation of the interaction of a pair of vortices with a free surface has been undertaken. The analysis is based on the vortex-sheet representation of the free surface and the use of the appropriate boundary conditions. The experiments were performed in a large basin and the vortices were generated through the use of a special nozzle. The rise of the resulting Kelvin oval, the trajectories of the vortices, and the instantaneous shape of the free surface were recorded on a video tape and then carefully analyzed through the use of a Motion Analysis system. The results have shown that the rise of the vortices not only gives rise to two scars, with a pronounced hump in the middle, but also, and more importantly, to a three-dimensional instability heretofore unknown. The measured and calculated vortex trajectories and the free-surface shapes at the corresponding times and Froude numbers are found to be in reasonable agreement. The new instability will form the basis of future investigations.

TABLE OF CONTENTS

LIST OF FIGURES

LIST OF SYMBOLS

b_o	Initial vortex pair spacing
N	Number of free surface vortices
d_o	Initial depth of the vortex pair
Fr	Froude Number
g	Gravitational acceleration
i	$\sqrt{-1}$
q_m	Scalar velocity $\sqrt{u^2 + v^2}$
t	Time
T	Nondimensional time ($V_o t/b_o - d_o/b_o$)
u	x-component of velocity
v	y-component of velocity
V_o	Initial or steady state mutual induction velocity
w(z)	Complex velocity function
x	Horizontal component of the coordinate axis (parallel to the line joining the vortex cores)
y	Vertical component of the coordinate axis
z_i	Complex position of a vortex
z_o	Complex position of the right-hand vortex in the vortex pair
$\bar{z}_i$	Complex conjugate of z_i
$\bar{z}_o$	Complex conjugate of z_o
δ	Desingularization parameter
Γ_N	Circulation of a given distributed vortex
Γ_o	Circulation of the vortex pair

η	Position of the free surface
η_m	$\frac{\eta}{L_c}$
ϕ	Velocity potential
ϕ_m	$\frac{\phi}{\Gamma_o}$
x_{max}	The maximum x/b_o position along the free surface
x_v	The x/b_o position of the center of the free surface vortex distribution
ρ	Density of water

ACKNOWLEDGMENTS

There is a good deal of humanism and humor available to a science teacher if he develops an intimate and flexible approach to his subject.

T. von Karman

The author wishes to express sincere appreciation to Distinguished Professor T. Sarpkaya, because he has subscribed to the above philosophy. An education is far more than academics, and creative impulses rather than memory must be trained for us to realize our potential in learning. For these lessons, and much more, I will respect and remember Professor Sarpkaya.

In addition, the author wishes to thank Mr. Jack McKay of the Mechanical Engineering Department Machine Shop for his creative genius and unending support throughout the experimental phases.

I. INTRODUCTION

This is part of continuing basic research toward the understanding of the fundamental mechanisms and physical processes underlying two- and three-dimensional vortex/free-surface interactions in homogeneous, stratified, and sheared media, taking into account ambient turbulence, viscous effects, and various large-scale instabilities (sinusoidal instability and vortex breakdown) for ship- and submarine-related hydrodynamics in a real ocean environment.

The name "remote sensing" was first used in the early 1960s, when it was recognized that the term "aerial photography" was no longer suitable to describe new kinds of images formed using energy outside the visible spectrum. The developments in 1970s (largely by NASA) gave rise to the development of a serious scientific interest in remote sensing. This interest led to the routine availability of multi-spectral data of large portions of the earth's surface. As far as the oceans are concerned, the interpretation and use of the multi-spectral data required a clear understanding of the physics of various phenomena leading to surface signatures resulting from the body-wake free-surface interaction in two- and three-dimensional, sheared, and/or stratified media, with or without ambient turbulence.

As far as the ship wakes are concerned, the most significant wake signature has been thought, for nearly a century, to be the Kelvin wave

pattern, with its 38.9° wake angle (see Figure 1). Observations made with remote sensing devices (e.g., synthetic aperture radar) have changed this perception dramatically and have shown clearly that a narrow strip of disturbed wake (scars and striations) exists for several hours behind the ship (see Figures 2a and 2b) with little or no sign of the Kelvin wake. These features have been termed turbulent wakes, although it is not clear that turbulence alone is responsible for their appearance. While the understanding of the physics of this phenomenon, through experimentation and numerical simulation, has attracted a great deal of attention, a satisfactory model describing the essential features of the radar images has not yet been presented. It appears that many competing and interacting processes are responsible for the observed scar and striation pattern. It has been suggested that vortices produced by the ship's hull may be responsible for the suppression of surface waves near the ship track and an enhancement of the waves near the edges of the smoothed area. Not only the free-surface signatures generated by the vortical flow but also the natural waves radiate energy away from the wedge-shaped wake region and thereby affect the flow itself. It appears that the dark, narrow images are visible due to a decrease in radar return (negative spectral perturbation) aft of a ship and not to an increase in radar backscatter along the edges of the wake.

The three-dimensional temporal development of the surface signatures resulting from the interaction of an ascending inclined vortex

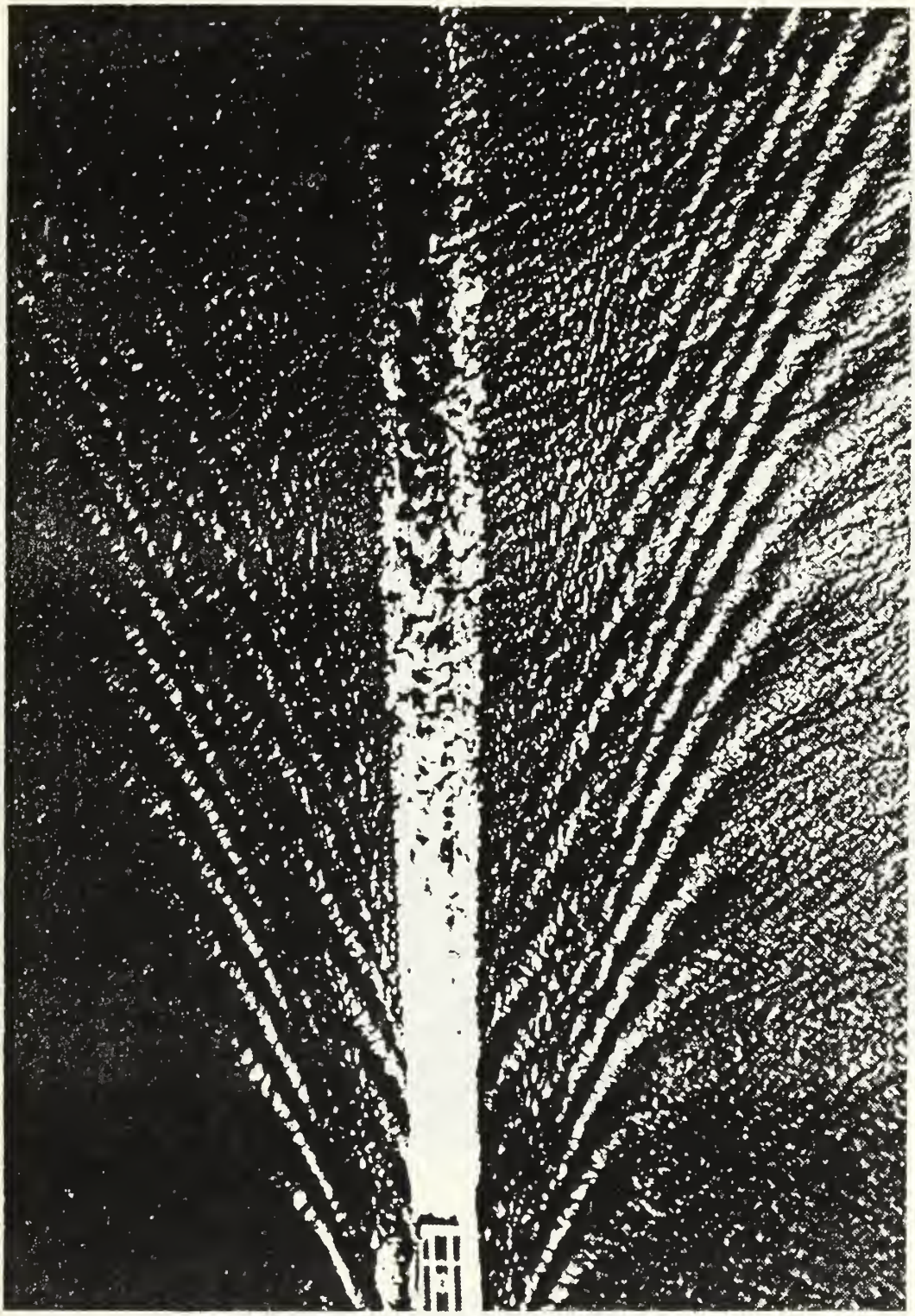

Figure 1. **Kelvin Waves and White-Water Wake of a Ship**

Figure 2a. **SAR Image of the Narrow Turbulent Wake of a Ship**

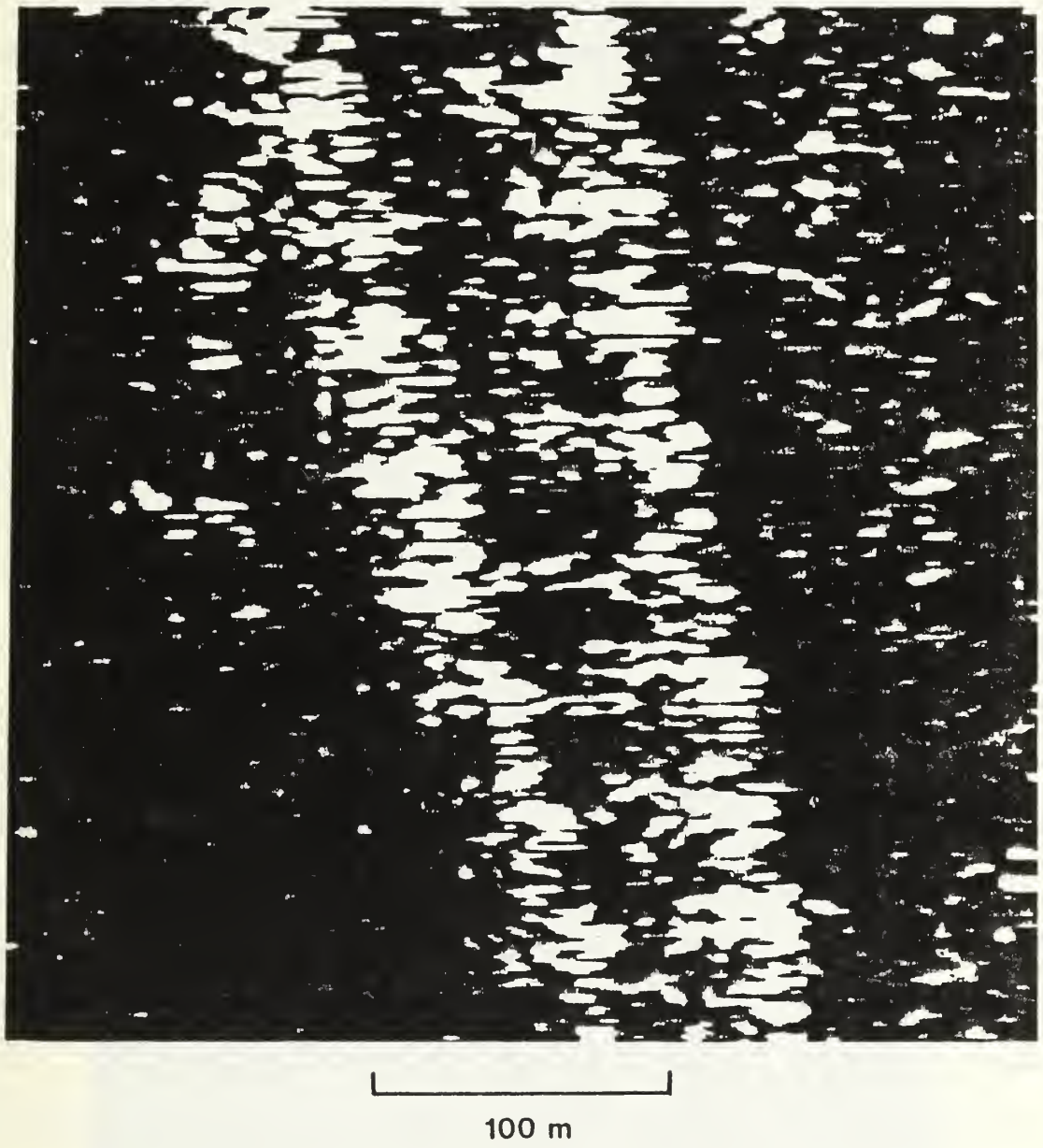

Figure 2b. **Close-Up View of the SAR Image of the Narrow Turbulent Wake of a Ship**

pair with the free surface was first described by Sarpkaya [Ref. 1] and Sarpkaya and Henderson [Ref. 2]. When a trailing vortex pair generated by a lifting surface approaches the free surface, with or without mutual induction instability and/or vortex breakdown, the vortices and/or the crude vortex rings give rise to surface disturbances (scars and striations, see Figures 3a and 3b). The striations are essentially three-dimensional free-surface disturbances, normal to the direction of the motion of the lifting surface, and come into existence when the vortex pair is at a distance equal to about one initial vortex separation from the free surface. The scars are small, free-surface depressions on either side of a nearly symmetrical hump, directly above the plane of symmetry of the vortex pair. They come into existence towards the end of the pure striation phase and when the vortices are at a distance equal to about sixty percent of the initial vortex separation (b_o) from the free surface. The scars are created and driven by the vortices and both move outward. Sarpkaya [Ref. 1] and Sarpkaya and Henderson [Ref. 2] found that the vortices diffuse rapidly and their circulation decreases slowly at first (prior to the occurrence of scars) and rapidly thereafter due to the counter-sign vorticity generated in the overlapping regions of the vortex pair in the recirculation cell and at the free surface.

Previous studies of a vortex (or vortex pair) in ground- or free-surface effect have been generally concerned with the boundary layer development, generation of oppositely-signed vorticity, the flow

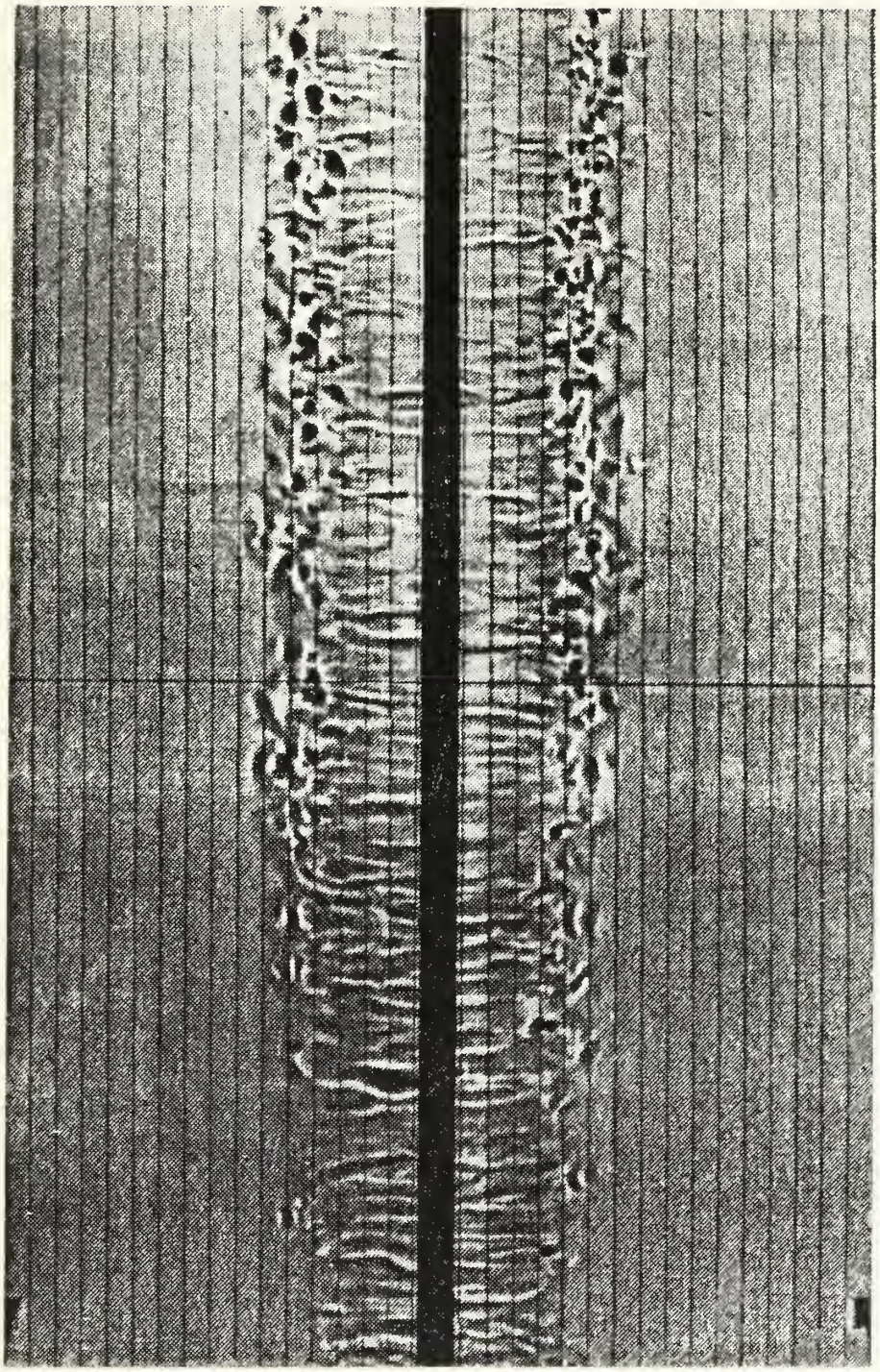

Figure 3a. **Scars and Striations Resulting From a Pair of Trailing Vortices**

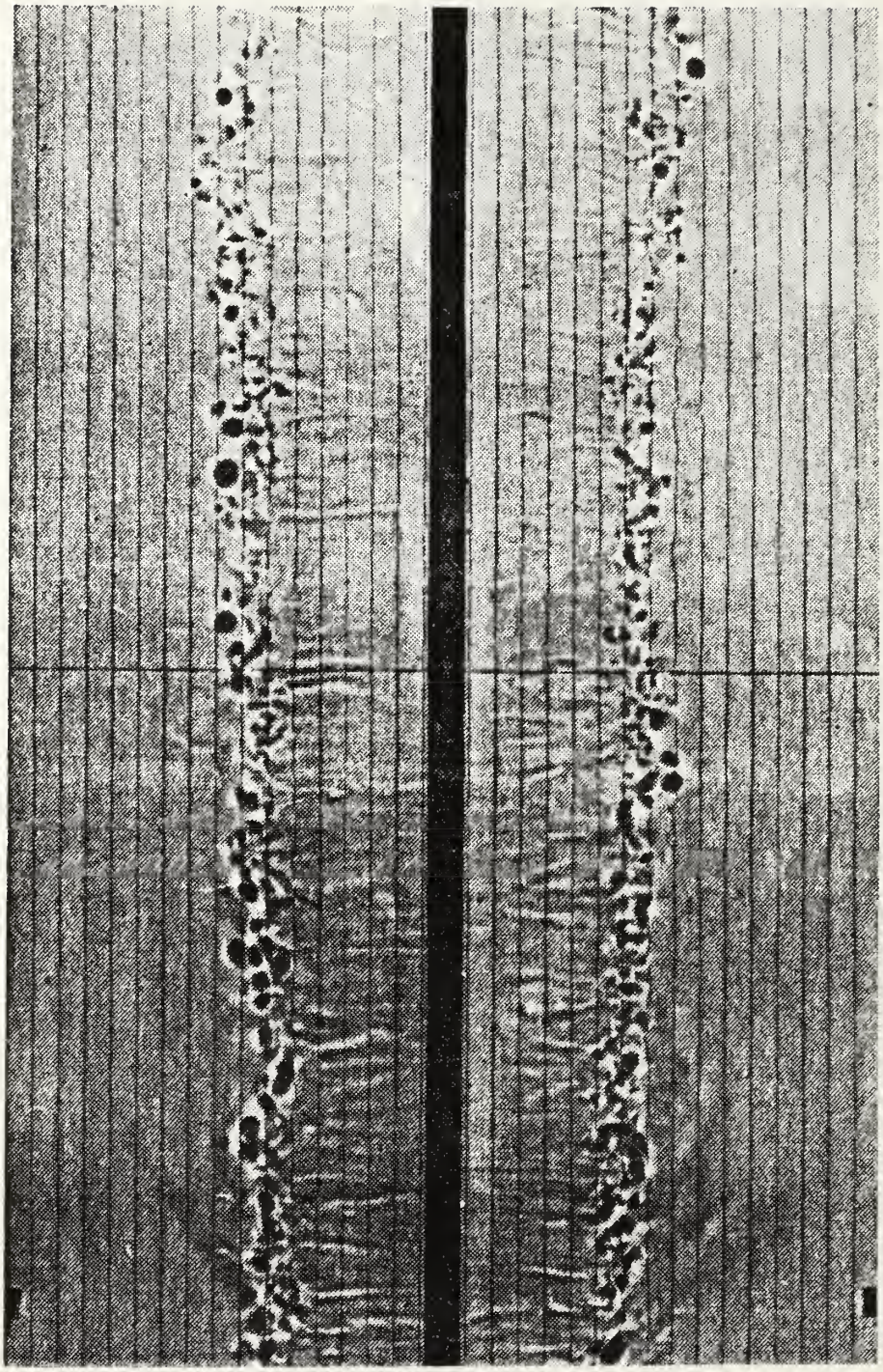

Figure 3b. **Scars and Vortical Structures Resulting From a Pair of Trailing Vortices**

resulting from a single vortex held fixed in a uniform flow, and the so-called "rebounding" phenomenon, according to which the vortices move at first toward the boundary, as on an inviscid trajectory, and then away from it [Refs. 3–6]. The boundary surface may be either a rigid boundary at which the no-slip condition is satisfied or a clean free surface corresponding to zero shear stress. In either case, the boundary surface gives rise to oppositely-signed vorticity and the net circulation of the vortices decreases with time [Ref. 5].

Sarpkaya and Henderson's [Refs. 1, 2] theoretical analysis of the scars created by the trailing vortices was based on the classical solution of Lamb [Ref. 7], assuming the vortices to be two-dimensional and the free surface to be a rigid plane. For small Froude numbers F ($F = V_o/\sqrt{gb_o}$, where V_o is the initial mutual induction velocity of the vortices and b_o is the initial vortex separation), each scar front was shown to coincide with the stagnation point on the Kelvin oval, formed by one of the pair of the trailing vortices and its image. For Froude numbers larger than about 0.15, not only the deformation of the free surface but also the nonlinear interaction between the said deformation and the motion of the vortices are significant. Thus, the free surface may no longer be assumed rigid. Even though it was fully realized at the outset that the problem to be ultimately solved is the understanding of the effects of three-dimensionality, shear, stratification, and the parameters characterizing the body-shape and motion on the evolution of the surface signatures, the relative ease of the study of the two-dimensional flow attracted the immediate attention of

experimentalists and numerical analysists alike in the past few years (Sarpkaya, et al. [Ref. 8]; Willmarth, et al. [Ref. 9]; Dahm, et al. [Ref. 10]; Marcus [Ref. 11]; and Telste [Ref. 12]).

Sarpkaya, et al.'s two-dimensional experiments were conducted in a 12-foot-long, three-foot-wide, and four-foot-deep (12' x 3' x 4') water basin. The nearly two-dimensional vortex pair was generated through the use of two counter-rotating plates. Neutrally buoyant fluorescent dye was used to visualize the flow. Sarpkaya, et al. [Ref. 8] also carried out a numerical analysis of the scars through the use of vortex dynamics. Their results have shown that the two-dimensional evolution of the free surface can be calculated (up to certain normalized times) through the use of line vortices or dipoles. The analysis becomes more robust as the Froude number is increased. At larger times, the results become unrealistic because the laminar and turbulent diffusion of vorticity are ignored. No wave train was observed on either side of the scars for any of the Froude numbers encountered in the analysis or experiments.

Willmarth, et al. [Ref. 9] and Dahm, et al. [Ref. 10], at the University of Michigan, adopted Sarpkaya, et al.'s [Ref. 8] idea of counter-rotating plates to generate vortices and carried out similar experiments on vortex-pair free-surface interaction. They too have used vortex methods to calculate the path of the vortices and the deformation of the free surface. However, no detailed comparisons were presented between the observed and calculated scar characteristics.

Marcus [Ref. 11], working with Berger at UC Berkeley, used the finite-difference method to investigate the inviscid, two-dimensional interaction between a pair of counter-rotating line vortices and a free surface. He has not conducted any experiments and encountered considerable numerical-stability problems at lower Froude numbers. At higher Froude numbers, his predictions were somewhat larger than those measured and calculated by Sarpkaya, et al. [Ref. 8]. Telste [Ref. 12] used vortex dynamics to investigate the same phenomenon (inviscid two-dimensional interaction between a two-dimensional vortex pair and the free surface). At medium and lower Froude numbers, his calculations required extensive numerical filtering to avoid or to delay numerical instability. The calculations are generally terminated when the free surface forms a sharp corner or when difficulties are encountered in obtaining rapid convergence. There does not seem to be any direct relation between the breakdown of the numerical model, breakdown of the waves, and the attainment of maximum scar conditions. Telste offered no comparisons with experiments.

It is clear from the foregoing that the investigation first initiated by Sarpkaya [Ref. 1] at the Naval Postgraduate School quickly mushroomed into a full-scale scientific effort on vortex/free-surface interactions, partly because of its intrinsic interest and partly because of its far-reaching practical applications in ship- and submarine-related hydrodynamics in a real ocean environment. It is also clear that much remains to be accomplished, both theoretically and

experimentally, toward the understanding of the evolution of surface signatures.

The present investigation has a two-fold purpose:

1. To conduct further parametric studies of the variables affecting the performance of the numerical model through the use of the vortex-sheet representation of the free surface; and

2. To investigate in greater detail the motion of a vortex pair approaching and intruding through the free surface and to delineate the characteristics of the scars and striations.

II. NUMERICAL SIMULATION

A. DESCRIPTION OF THE MODEL

The flow model consists of two counter-rotating vortices (CRVs) of constant circulation, moving towards the free surface, and a vortex sheet, represented by a number of equi-spaced line vortices at the free surface. The model is a generalized boundary integral/vortex method developed by Baker, Meiron and Orszag [Ref. 13].

The use of Bernoulli's equation on either side of the fluid interface leads to

$$\frac{\partial \phi_1}{\partial t} + \tfrac{1}{2}(u_{t1}^2 + u_{n1}^2) + g\eta_1 + \frac{p_1}{\rho_1} = F_1(t) \tag{1a}$$

and

$$\frac{\partial \phi_2}{\partial t} + \tfrac{1}{2}(u_{t2}^2 + u_{n2}^2) + g\eta_2 + \frac{p_2}{\rho_2} = F_2(t) \tag{1b}$$

in which ϕ is the velocity potential, u is velocity, g is gravitational acceleration, t is time, η is surface elevation above mean water level, ρ is density, p is pressure, s is distance along surface, the suffixes t and n denote components tangential and normal to the surface, and the suffixes 1 and 2 denote the lower and upper surface. Furthermore, on the surface one has

$$p_1 = p_2 = p$$

$$u_{n1} = u_{n2} = u_n$$

$$\eta_1 = \eta_2 = \eta$$

$$\gamma_t = u_{t1} - u_{t2}$$

$$u_t = (u_{t1} + u_{t2})/2 \qquad (2)$$

$$U = (u_1 + u_2)/2$$

$$V = (v_1 + v_2)/2$$

$$\Gamma = \gamma_t \, ds = \gamma dx$$

The use of the foregoing plus the free surface condition given by

$$\frac{D\phi}{Dt} - \frac{1}{2}(\phi_x^2 + \phi_y^2) + F^{-2}\eta = 0 \qquad (3)$$

lead [Ref. 14] to the momentum equation for the calculation of the evolution of vorticity

$$\frac{\partial \gamma}{\partial t} = -\frac{\partial}{\partial x}(U\gamma) + 2At\left[\frac{\partial U}{\partial t} + U\frac{\partial U}{\partial x} + \left(\frac{\partial V}{\partial t} + U\frac{\partial V}{\partial x}\right)\frac{\partial \eta}{\partial x}\right.$$

$$\left. + \frac{C^2\gamma}{4}\left(\frac{\partial \gamma}{\partial x} - CS\gamma\frac{\partial^2 \eta}{\partial x^2}\right) + g\frac{\partial \eta}{\partial x}\right] \qquad (4)$$

where the Atwood number $At = (\rho_2 - \rho_1)/(\rho_2 + \rho_1)$. For the air/water interface, $At = -1$.

The velocity of a vortex may be decomposed into two parts: One stemming from the use of line vortices (i.e., the two CRVs and the surface vortices, equi-spaced at mid-points of the segments) and the other from the corrections to the first due to the distributed nature of vorticity along the sheet. Thus one has:

$$U_k/V_o = (U_1 + U_2)/V_o \qquad (5a)$$

$$V_k/V_o = (V_1 + V_2)/V_o \qquad (5b)$$

where the U_1 and V_1 components of velocity are obtained from the complex function w(z). Normalizing the strengths of all vortices by the strength of the counter-rotating vortex pair, all velocities by V_o (= $\Gamma_o/2\pi b_o$), and all distances by b_o, one has

$$w = \frac{1}{i}\ln(z - z_o) - \frac{1}{i}\ln(z + \bar{z}_o) - \sum_{k=1}^{m}\frac{1}{i}\Gamma_k \ln(z - z_k) + \sum_{k=1}^{m}\frac{1}{i}\Gamma_k \ln(z + \bar{z}_k) \qquad (6)$$

in which z_o and $-\bar{z}_o$ are the positions of the CRVs and z_k and $-\bar{z}_k$ denote the positions of the free surface vortices. The velocities U_1 and V_1 are then given by

$$(U_1 - i\,V_1)/V_o = dw/dz \qquad (7)$$

and the velocity components U_2 and V_2 are given by [Ref. 14]

$$U_2 = \frac{\Delta x}{2\pi}\left(\frac{\partial\gamma}{\partial x}\cdot\frac{\partial\eta}{\partial x} + \frac{\gamma}{2}\frac{\partial^2\eta}{\partial x^2}\right)_k \qquad (8a)$$

$$V_2 = -\frac{\Delta x}{2\pi}\left(\frac{\partial\eta}{\partial x}\right)_k \qquad (8b)$$

From a mathematical point of view, one would like to have the free surface extend from $-\infty$ to $+\infty$ and the CRVs originate at (0.5, $-\infty$) and at (-0.5, $-\infty$). This is impossible from a numerical point of view. It is necessary to obtain guidance from experiments to limit the computer time. Observations have shown that the free surface rises in a

relatively small region directly above the CRVs and no waves are generated beyond the scars (see Figure 4). In fact, the linearized analysis of Kochin, et al. [Ref. 15] of the motion of a line vortex under a free surface has shown that the resulting steady wave train far from the vortices would be negligibly small. The sample calculations led to the conclusion that the free surface can be restricted to a region extending from $x = -10$ to $x = +10$. Furthermore, the CRVs are assumed to originate at a depth of $y = -5$, in view of the fact that the free surface does not begin to deform until the CRVs arrive at about $y = -1$.

Theoretically, one can calculate the potential function ϕ from the complex velocity potential w, the velocity of the vortices from $dw/dz = u-iv$ (excluding the vortex whose velocity is being calculated), and the elevation of the free surface from equations 3 or 4 for a given Froude number, and trace the evolution of the free surface as a function of time. This relatively simple-sounding procedure is anything but simple, primarily because the numerical short-wavelength instabilities eventually lead to large-scale instabilities. The critical time for the onset of these instabilities decreases with decreasing Froude number. It is because of this reason that the preliminary calculations were initially restricted to large Froude numbers. To be sure, the instability is not limited to boundary-integral methods. It is also an inherent characteristic of the space discretization methods. In fact, the choice of a particular method depends, more or less, on the user's past experience, the availability of a computer code, the objectives of the

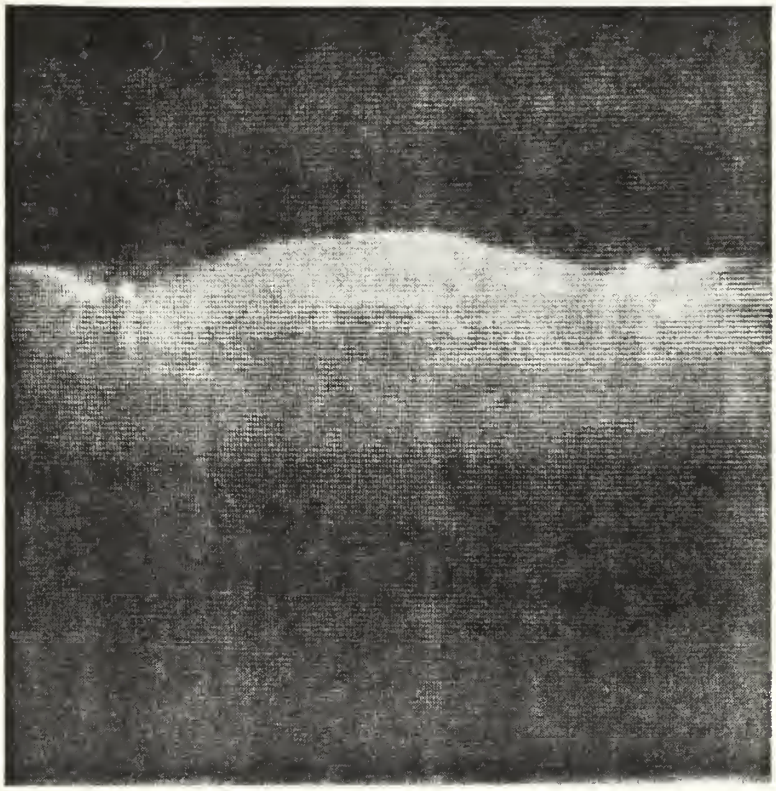

Figure 4. **Photograph of a Typical Free-Surface Deformation**

investigation, and the particular problem. A lucid discussion of the advantages and disadvantages of various techniques is presented by Yeung [Ref. 16]. Previous investigators dealing with marching methods for nonlinear water wave problems have used various filtering [Ref. 17] or regridding techniques to eliminate or delay the instability. In general, it is not easy to assess the accuracy of the results. Sensitivity analysis, parametric studies, and comparison with experiments may help to assess the error introduced by numerical smoothing and filtering techniques [Ref. 18]. One must also bear in mind that the numerical model might not necessarily correspond to a physically realizable flow (turbulent diffusion, axial instabilities, wall effects, etc.). In the present investigation, it was decided to use Rosenhead's [Ref. 19] smoothing technique, according to which any complex velocity is, in general, desingularized by introducing a cut-off distance δ, given by (see also Sarpkaya [Ref. 18]):

$$u_j - iv_j = \frac{1}{2i\pi} \sum \frac{\Gamma_k}{z_j - z_k} \frac{|z_j - z_k|^2}{|z_j - z_k|^2 + \delta^2} \tag{9}$$

The use of other smoothing techniques (e.g., the Longuet-Higgins and Cokelet technique [Ref. 17]) was rejected because it tends to oversmoothen the free surface. Furthermore, as argued by Roberts [Ref. 20], the five-point scheme of Longuet-Higgins and Cokelet may lead to hopelessly large errors in some applications. According to equation 6, the solution should approach the inviscid flow solution as $\delta \rightarrow 0$. Numerous calculations have shown that a $\delta/\Delta x$ value between 1.1

and 1.5 yields nearly identical results. The final calculations were performed using $\delta/\Delta x = 1.25$.

The specific details of the numerical calculations are as follows: (i) calculate the strength of the vortex sheet and the strength of the surface vortices by iteration until $\partial\gamma/\partial t$ and/or $\partial U/\partial t$ and $\partial V/\partial t$ converge to an acceptable limit, (ii) find the velocity of all vortices (including those of CRVs) and convect them for a time interval Δt using a second order modified Eulerian convection scheme ($\Delta t = 0.01$ in the calculations), (iii) calculate the area between the free surface and the x axis, and (iv) repeat the above steps. The procedure described above is relatively simple and does not require excessive computer time (about 30 minutes on IBM 3033). However, the free surface eventually does become unstable. The instability shows up as a kink in the free surface caused by the propensity of the neighboring vortices to orbit about each other. Some of the instabilities can be alleviated without smoothing. Initial calculations have shown that the vortices near the y axis begin to slide sideways as the free surface (or the vortex sheet) stretches. Consequently, the thinly populated regions of the sheet do not yield a smooth surface and the flow begins to leak between the vortices. Also, the regions where the free surface is depressed (where the scars develop) become overpopulated with vortices, leading to the growth of short-wavelength Helmholtz instability. This problem can easily be alleviated either by packing the vortices more densely near the y axis at the start of the calculations, so that the entire surface becomes more or less uniformly represented at later times, or by rediscretizing

the vortex sheet at suitable time intervals. This latter technique has been used in the present calculations (for additional details see Sarpkaya and Shoaff [Ref. 21]).

B. RESULTS OF THE NUMERICAL CALCULATIONS

Numerous runs were made at various Froude numbers from 0.35 to 0.65. In each case, the calculations were carried out until the instabilities were strong enough to cause a numerical floating point overflow error at some point during the execution of the program. A numerical filter was not used to eliminate or to delay the instabilities. Nondimensional time was used as well as nondimensional lengths and speeds. For the sample results shown here, the counter-rotating vortices were placed at $d_o/b_o = 3$. The start of their motion, measured by $T = (V_o t/b_o - d_o/b_o)$, was $T = -3$. The free surface was not allowed to start to deform until the vortex pair was within 2.5 units of the free surface. Horizontal placement of the vortex pair was at –0.5 and 0.5 units so that the distance between the two would be b_o.

Figures 5 through 8 show the evolution of the free surface at representative times for a Froude number of 0.53. The corresponding velocity-vector plots are shown in Figures 9 through 12. The path of the main vortex follows the path of a vortex pair approaching a rigid boundary until about $T = -1.6$. Then it starts to diverge and, instead of turning to the right as in the case of the rigid wall, it starts to move to the left very slowly. This is because the strengths of the discrete vortices placed near the center line are inducing a horizontal velocity

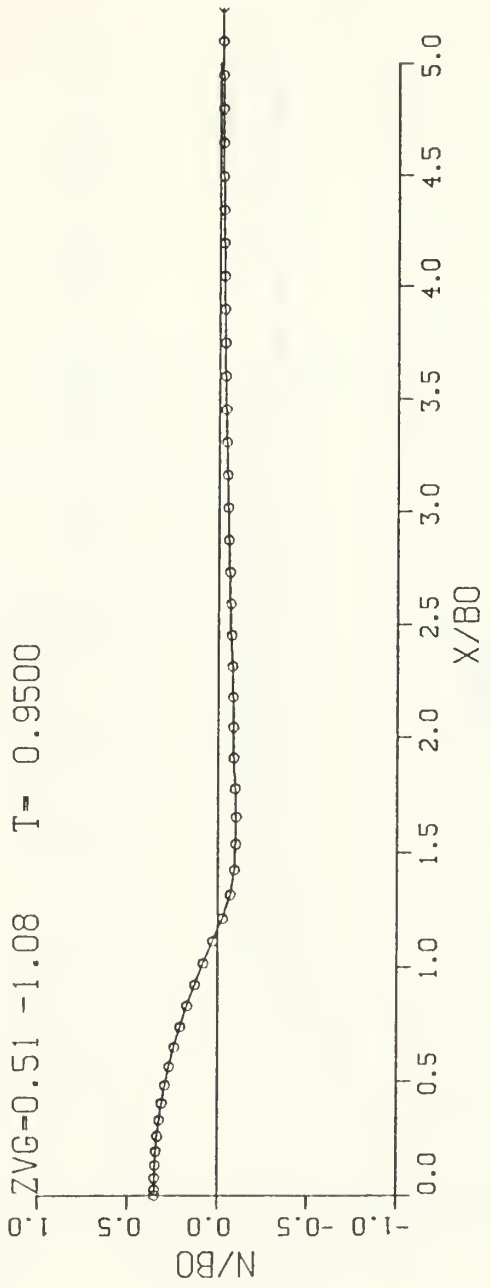

Figure 5. **Evolution of Free Surface at T = 0.95**

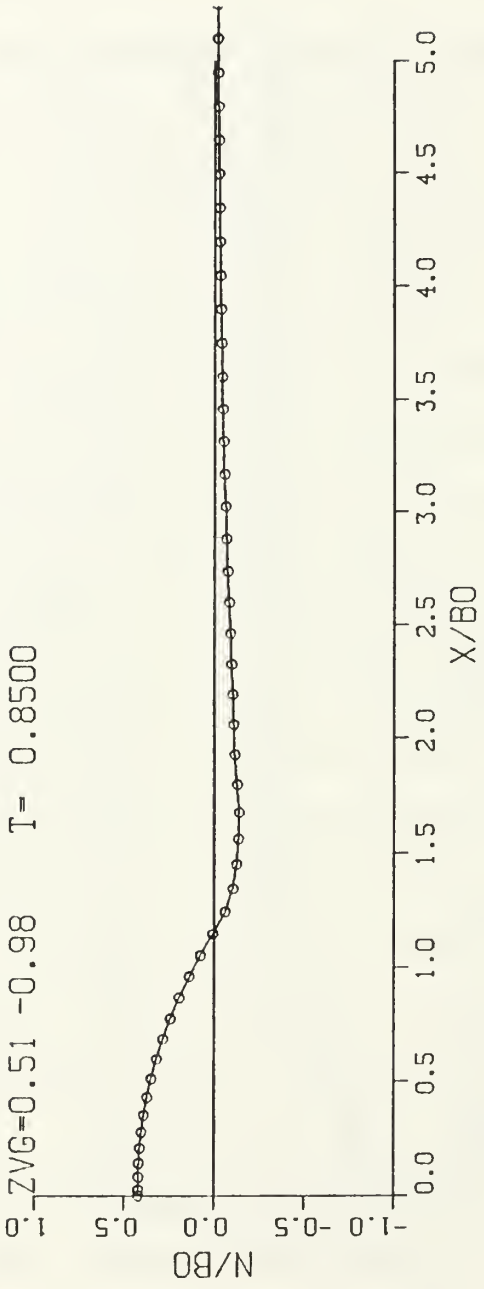

Figure 6. **Evolution of Free Surface at T = 0.85**

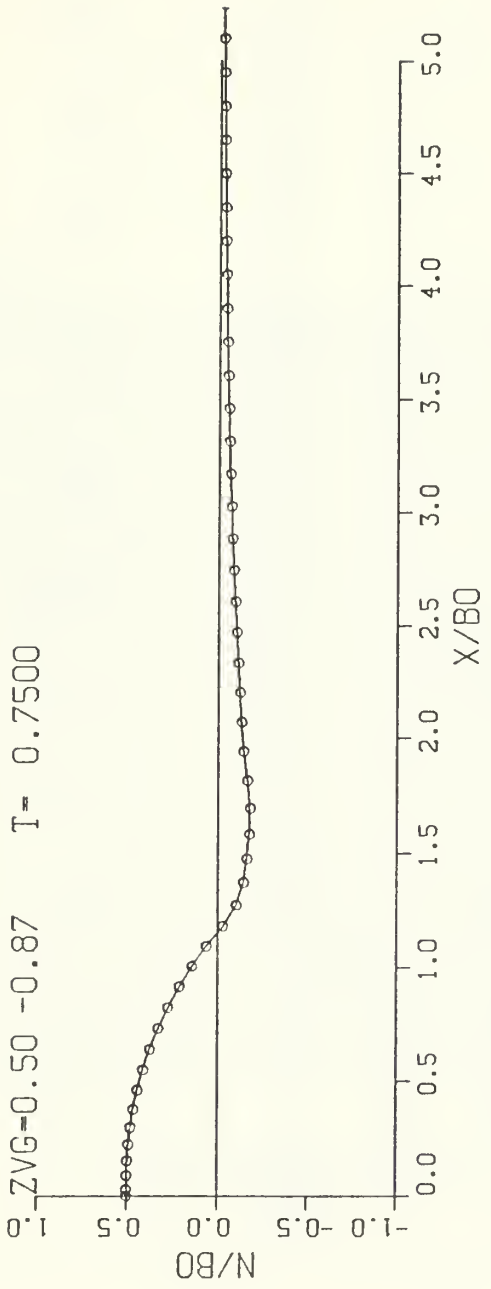

Figure 7. **Evolution of Free Surface at T = 0.75**

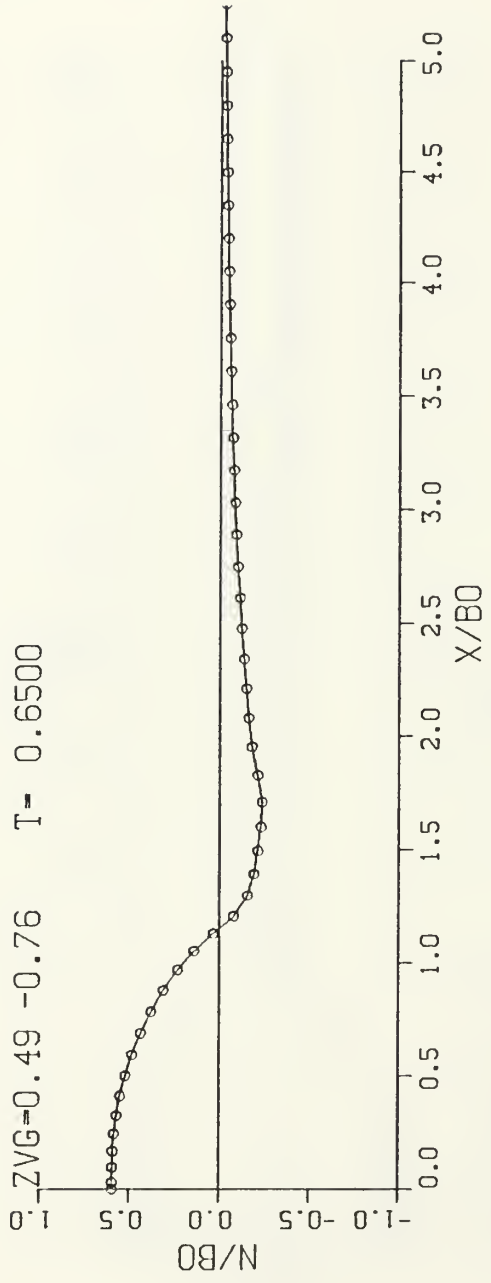

Figure 8. **Evolution of Free Surface at T = 0.65**

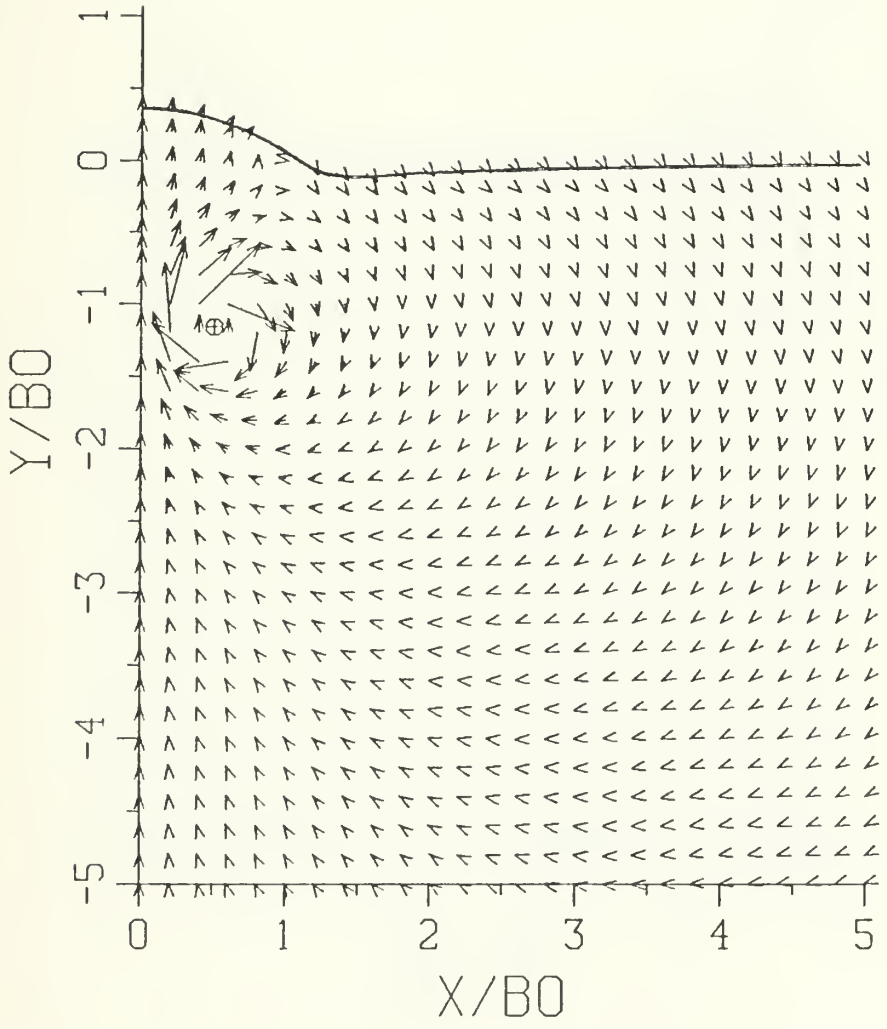

Figure 9. **Velocity Field at T = 0.95**

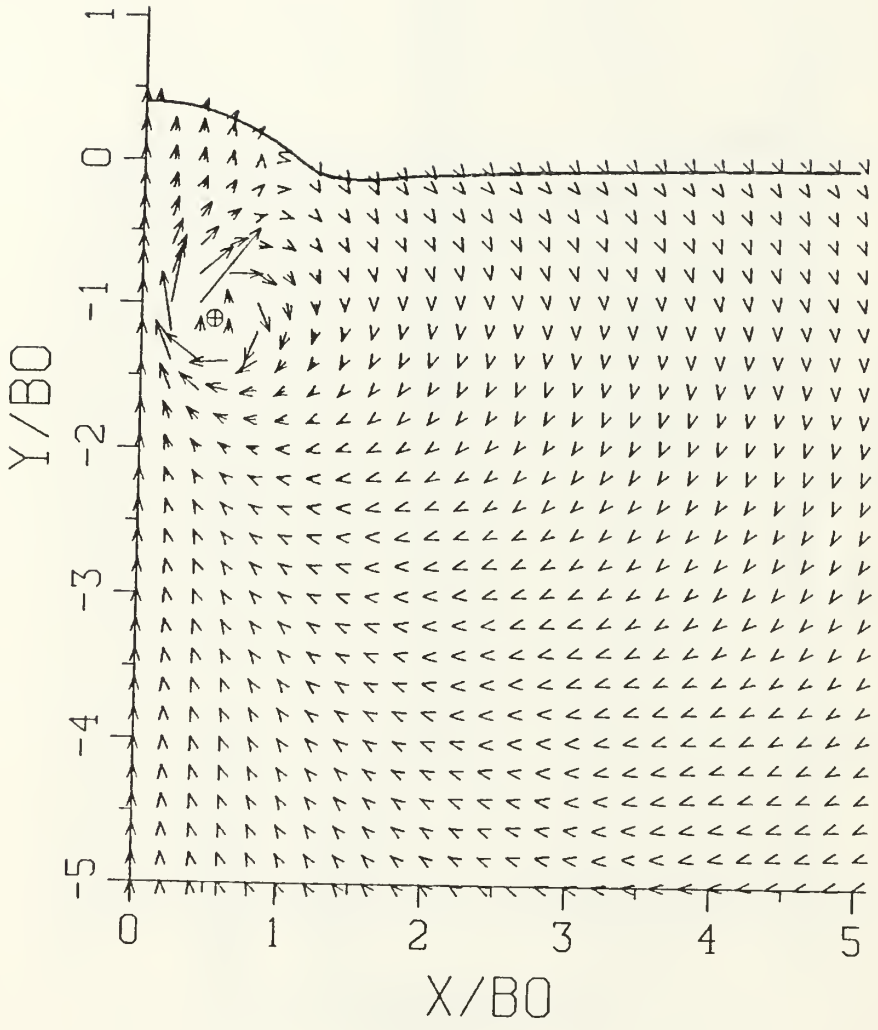

Figure 10. **Velocity Field at T = 0.85**

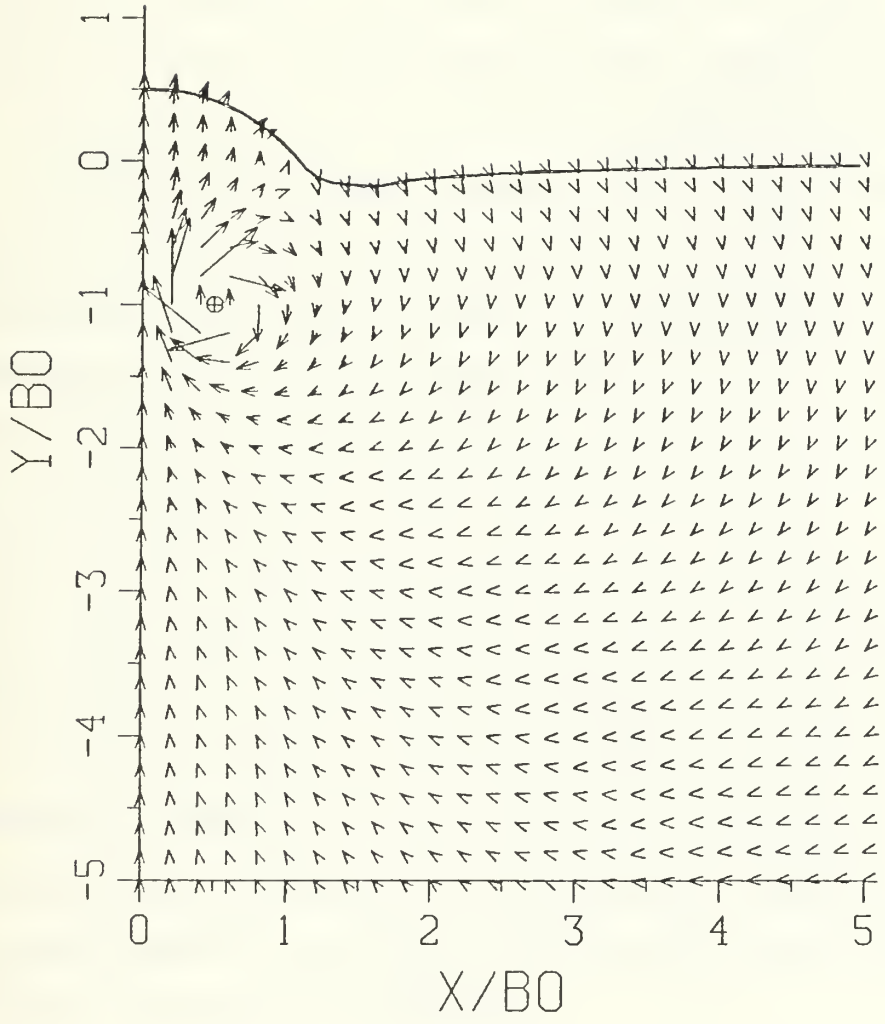

Figure 11. **Velocity Field at T = 0.75**

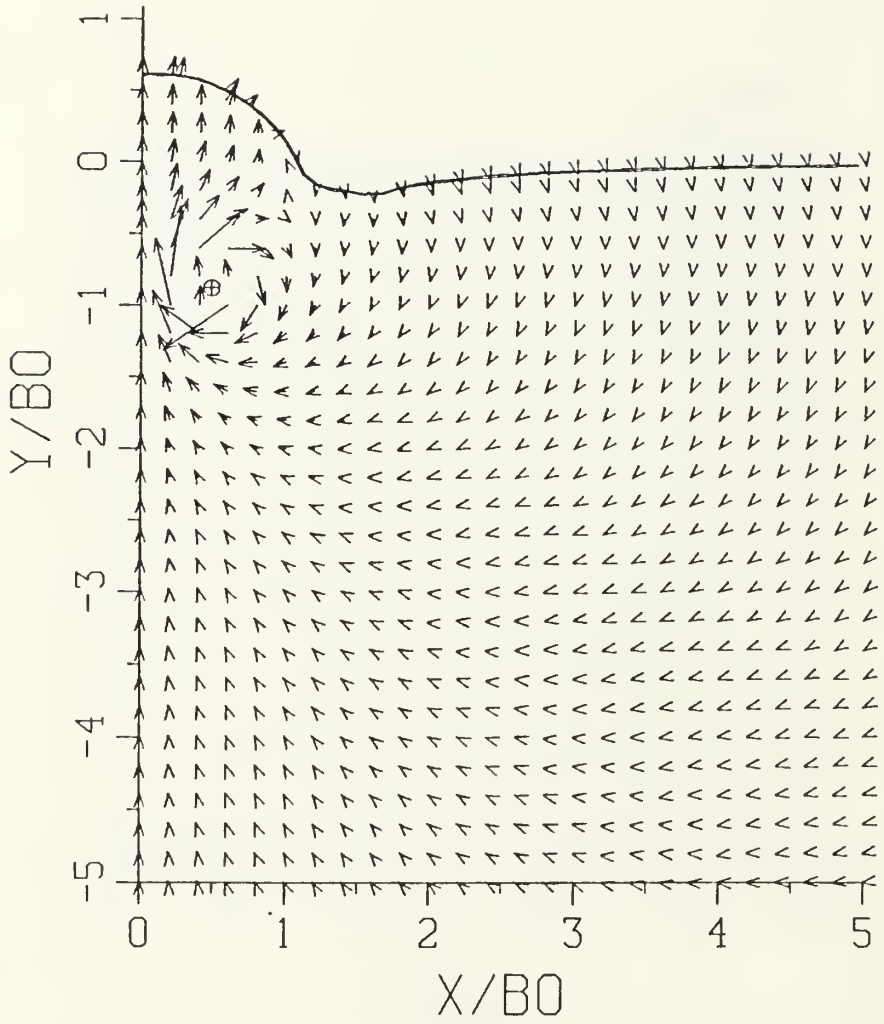

Figure 12. **Velocity Field at T = 0.65**

component to the left. This eventually would lead to the vortex moving up into the domed area underneath the free surface if the calculations had proceeded further. Figure 13 shows a sample plot of the streamlines, corresponding to the maximum time at which the calculations remained stable. It is important to note that the results cited above have not been subjected to any kind of numerical filtering. The calculations are generally terminated when the free surface forms a sharp corner or when difficulties are encountered in obtaining rapid convergence. There does not seem to be any direct relation between the breakdown of the numerical model and the attainment of maximum scar conditions. This is partly because the effect of viscous and turbulent diffusion on the counter-rotating vortices and on the scars and striations is not yet taken into account. Nevertheless, the idealized model gives some indication of the surface deformation and validates the conclusion that the rise of the vortex pair does not give rise to waves on either side of the scars, as anticipated by Kochin, et al. [Ref. 15]. Finally, it is clear that a two-dimensional numerical model cannot predict the existence of striations which are essentially three-dimensional instabilities. It is quite possible that the most important physical phenomenon leading to the existence and explanation of the dark narrow regions of wake behind the ships may be the striations or the interaction of striations with scars.

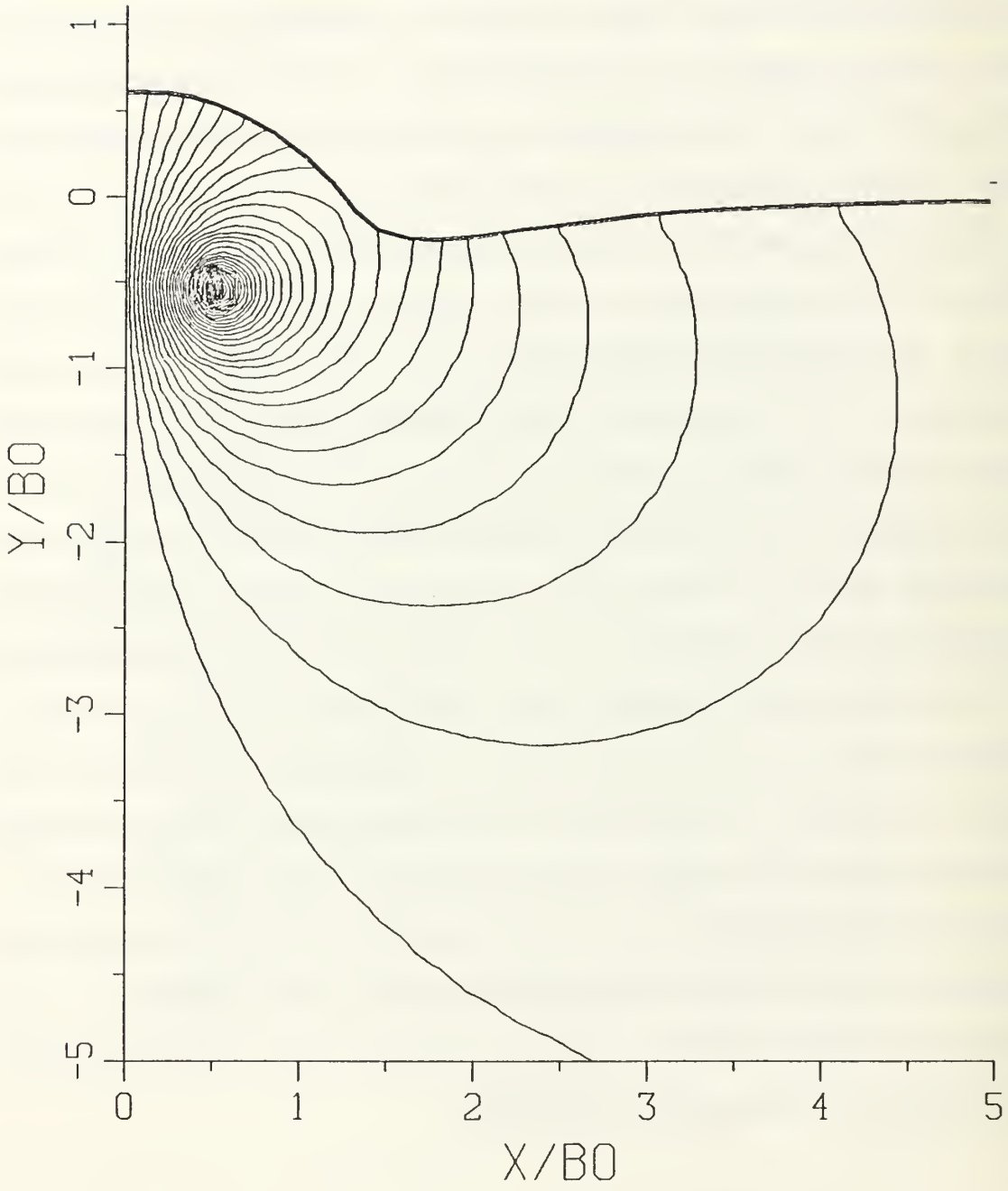

Figure 13. **Streamlines at T = 0.65**

III. EXPERIMENTS AND COMPARISONS

A. EXPERIMENTAL APPARATUS

Experiments were conducted in a water basin which was twelve feet long, three feet wide, and four feet deep. Additional details of the basin are described by Leeker [Ref. 22] and will not be repeated here.

Two-dimensional trailing vortices were generated through the use of three different methods:

1. The use of two counter-rotating plates which, when fully rotated, were flush with the bottom of the tank, i.e., they have "vanished" at the end of their rotation, as far as the resulting fluid motion is concerned (see Figure 14), and no secondary vortices were generated.

2. The use of a two-dimensional, sharp-edged slot on the wall of a chamber, attached to the bottom of the basin. The fluid in the chamber is driven by a piston, attached to a pulley and weight system.

3. The use of a streamlined nozzle attached to the aforementioned chamber, directly in front of the nozzle. Most of the experiments were conducted through the use of the nozzle because of the superior quality of the resulting vortices.

To visualize the flow created by the vortices, a fluorescein dye was introduced either from the false bottom at about the midpoint of each rotating plate or from the inner walls of the nozzle. The dye was controlled by making it slightly buoyant with the use of alcohol and by using a flow control valve just outside the tank near the dye exit.

Figure 14. **Rotating Plates and the Kelvin Oval**

The data collection system consisted of a video camera, a VHS video cassette recorder, a monitor, and a date/timer. The date/timer was used to imprint on the screen and the tape a running clock and date (which was used as a run number) for each experiment.

B. PROCEDURES

The tank was first filled to a suitable level and allowed to sit until the fluid had come to rest. Water levels were varied throughout the experimentation to assess the effect of the water level on how soon the vortices became turbulent. While waiting for the fluid to come to rest, the plates were opened and the weights set. After the fluid was at rest, the dye was slowly introduced into the system. When the dye had risen just above the tips of the plates, the collimated light source was turned on and the video recording system was set to run. The weights were then actuated, causing the plates to rotate, which created the two-dimensional vortices. The vortices rose by their mutual induction velocity. As the vortices continued to rise, the free surface started to deform, leading to the formation of scars and striations.

C. DATA ACQUISITION SYSTEM

A NEC TI-22P CCD camera was used to record the experimental runs onto a Panasonic AG-6300 Video Cassette Recorder. The VHS recorder is required because for every frame of video information displayed on the monitor, the VHS tape stores another frame of

information digitally which can later be extracted with the proper equipment. A Sun[1] computer with a motion analysis VP110 system was used to analyze the data. The motion analysis system allows the user to superimpose on the video monitor an outline of areas that have the same intensity or brightness levels. The brightness or area to be outlined is controlled by the user as he sets a threshold. The threshold can be varied from zero (black) to 1999 (white). The area outlined shows up on the monitor, allowing the user fine control of what is to be picked up by the computer.

The outlines are then turned into digital data and retained in a file by pixel location of the monitor screen. Once the data is stored, it can be edited and manipulated to eliminate unwanted images (see Figures 15a and 15b). Further manipulation then allows the user to find centroids of areas, paths of centroids, and velocity and acceleration of the particles on these paths. This is all done through the use of the software provided in a package known as ExpertVision.[2]

Figures 16 and 17 show the evolution of the free surface, as determined through the use of the ExpertVision, for the Froude numbers of Fr = 0.39 and 0.53. Also noted in these figures are the positions of the counter-rotating vortices. These will later be compared with those predicted numerically.

---

[1]Sun is a registered trademark of Sun Microsystems, Inc.

[2]ExpertVision is a registered trademark of Motion Analysis Corporation.

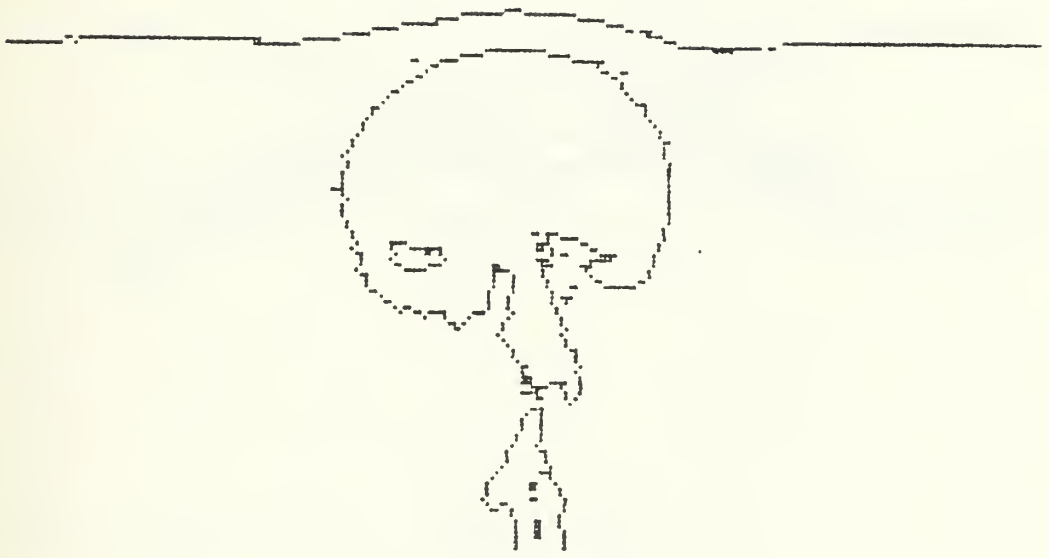

Figure 15a. **Identification of the Free Surface and the Kelvin Oval (early stages)**

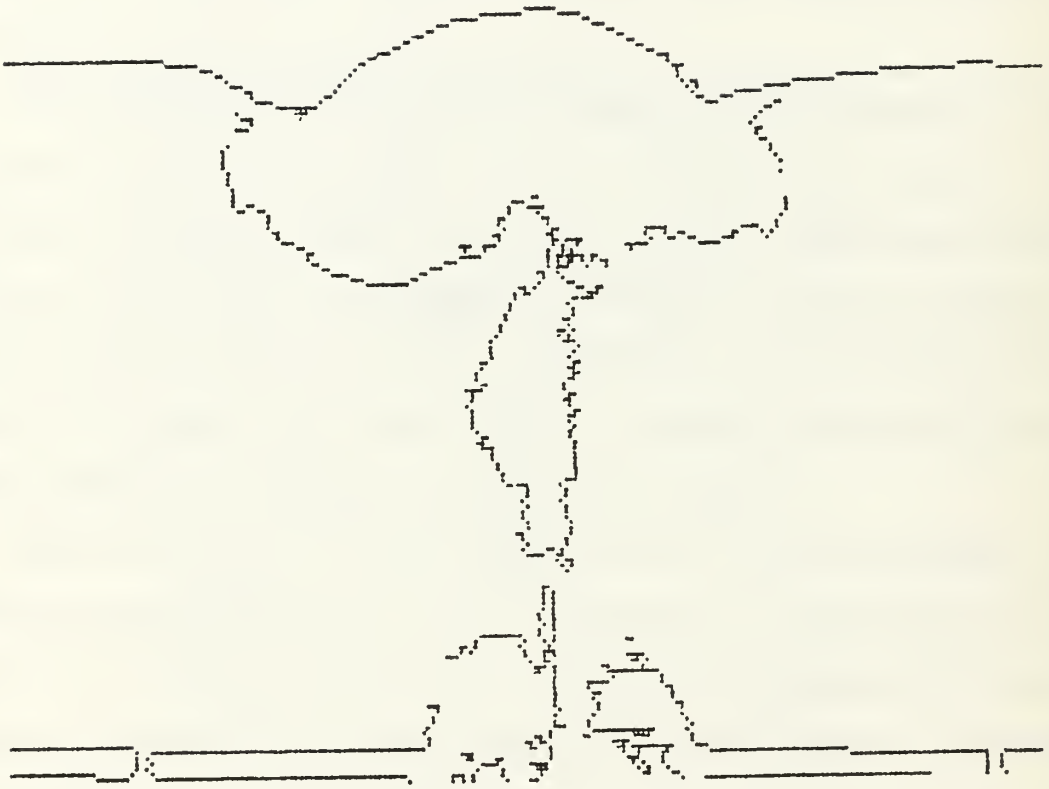

Figure 15b. **Identification of the Free Surface and the Kelvin Oval (later stages)**

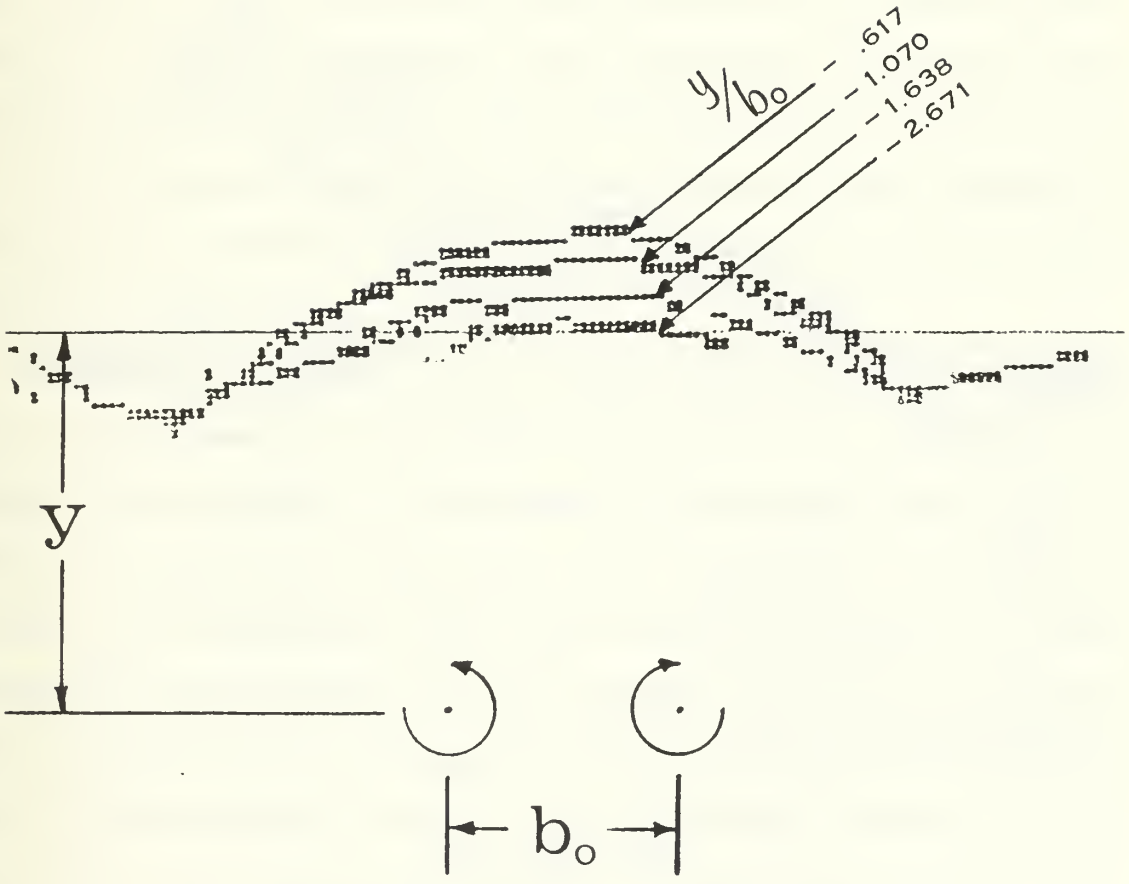

Figure 16. **Evolution of the Free Surface During the Rise of Vortices for Fr = 0.39**

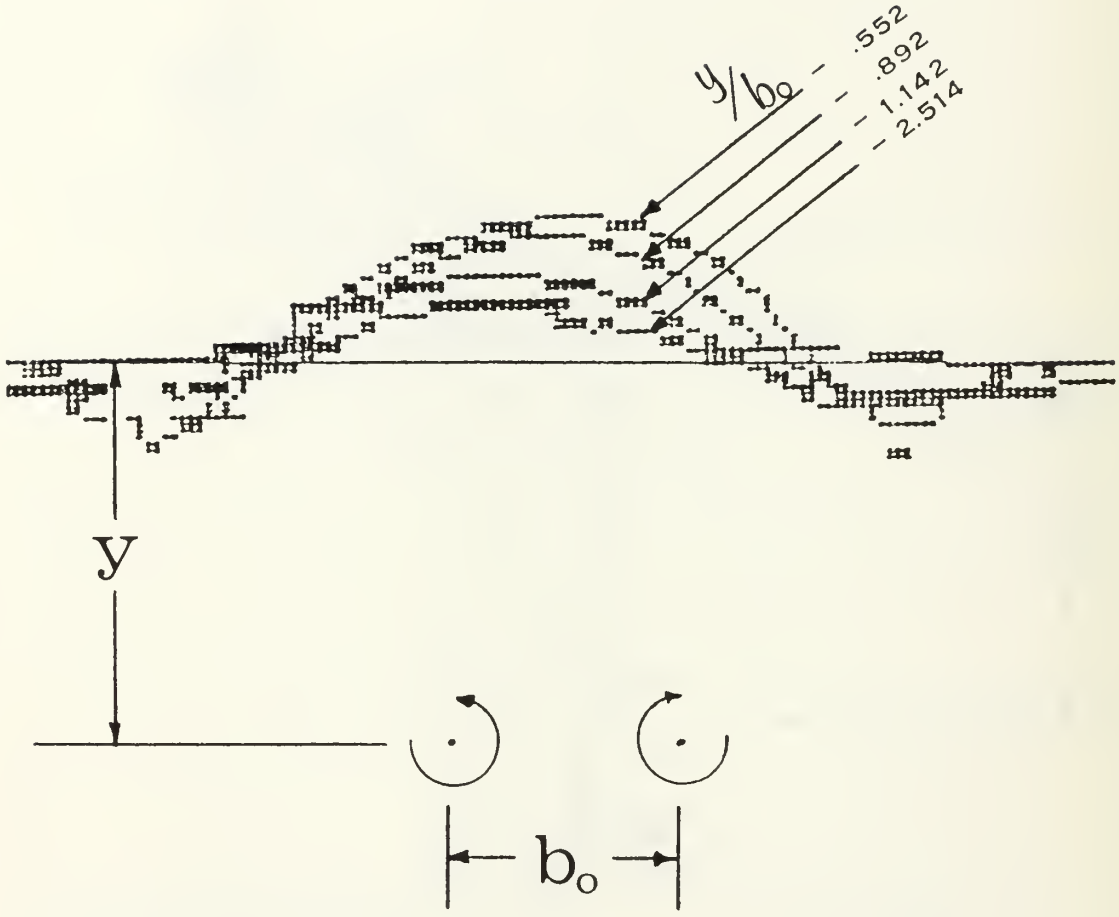

Figure 17. **Evolution of the Free Surface During the Rise of Vortices for Fr = 0.53**

D. COMPARISON OF ANALYSIS AND EXPERIMENTS

In general, the numerical model predicted closely several features that occurred in the experiments: the free surface shape, particularly the scar region and the smooth shape of the hump or domed area in the center. Furthermore, the model predicted that little would happen beyond $y/b_o = 3$. This was found to be true for the stages of deformation up until the time when the vortices lost nearly all of their vertical movement. The model also predicted the location of the scars to a high degree of accuracy as well as the slight inward movement of the path of the vortices during their vertical ascent as they are drawn into the humped region.

Figures 18 through 20 show a comparison of the variation of the local maximum of the free-surface deformation as a function of the instantaneous position of the counter rotating vortex pair for Fr = 0.39, 0.42, and 0.53, respectively. Where applicable, the agreement between the experimental data and numerical predictions is quite satisfactory, particularly when one considers the fact that the surface deformations take place in a time period less than 0.3 seconds and the fact that the numerical model is an inviscid flow idealization of our conceptual view of the phenomenon. The smaller the number of vortices or marker elements, the larger the dome height and slower the onset of the numerical instability. This is neither surprising nor entirely unexpected. The stability of vortex sheets and, in particular, the Helmholtz instability have been the subject of intense interest. It is

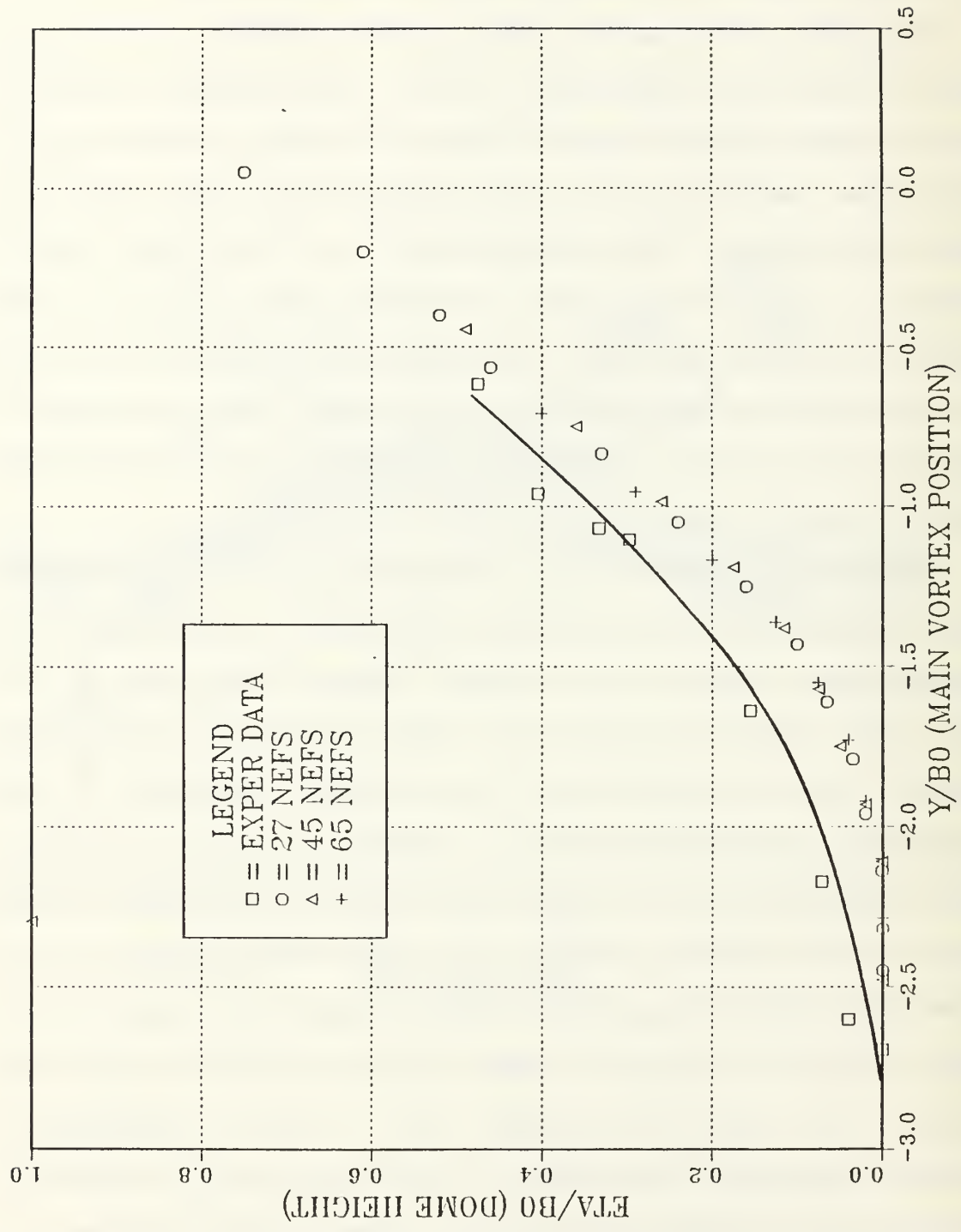

Figure 18. **Comparison of the Measured and Predicted Scar Elevations for Fr = 0.39**

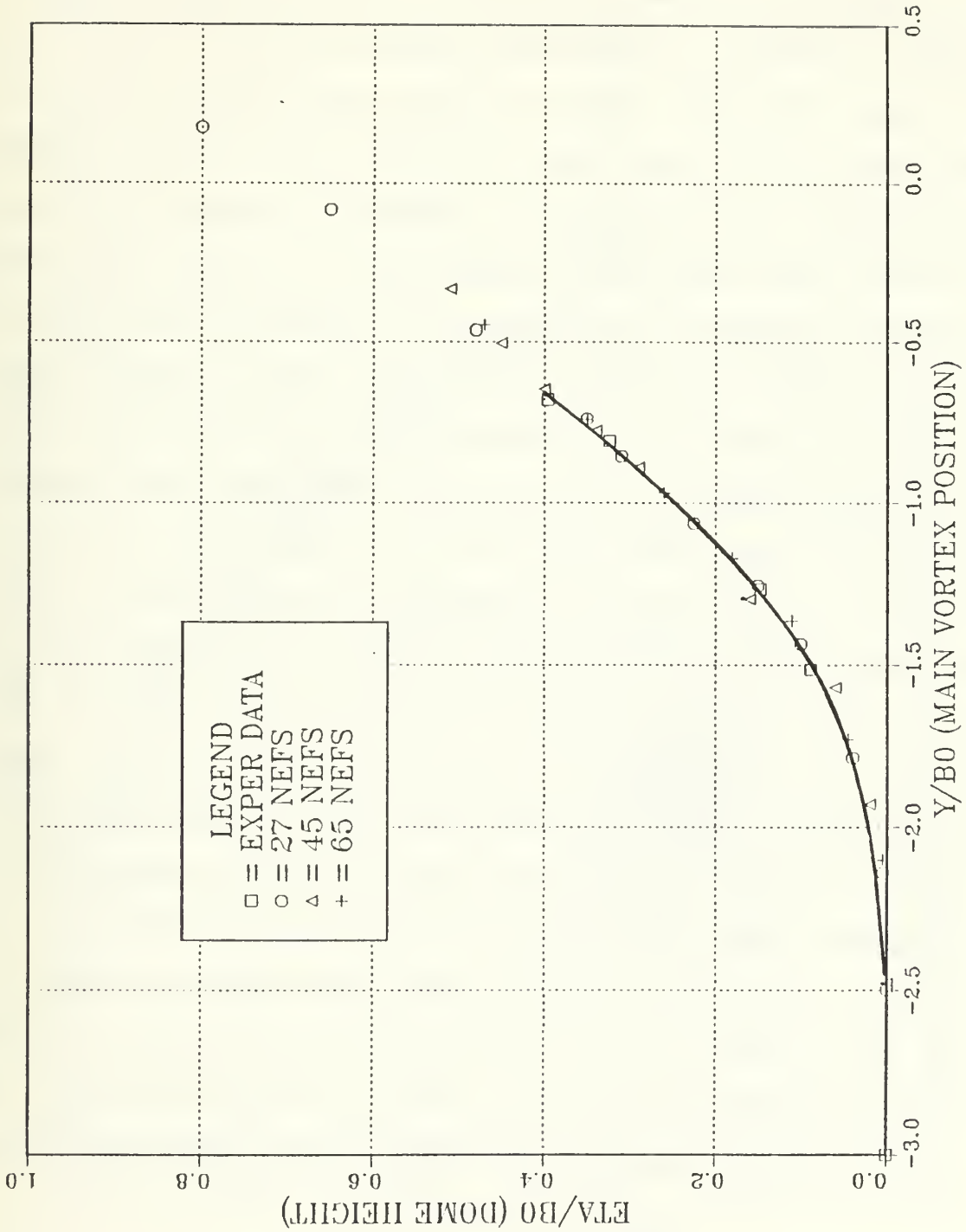

Figure 19. **Comparison of the Measured and Predicted Scar Elevations for Fr = 0.42**

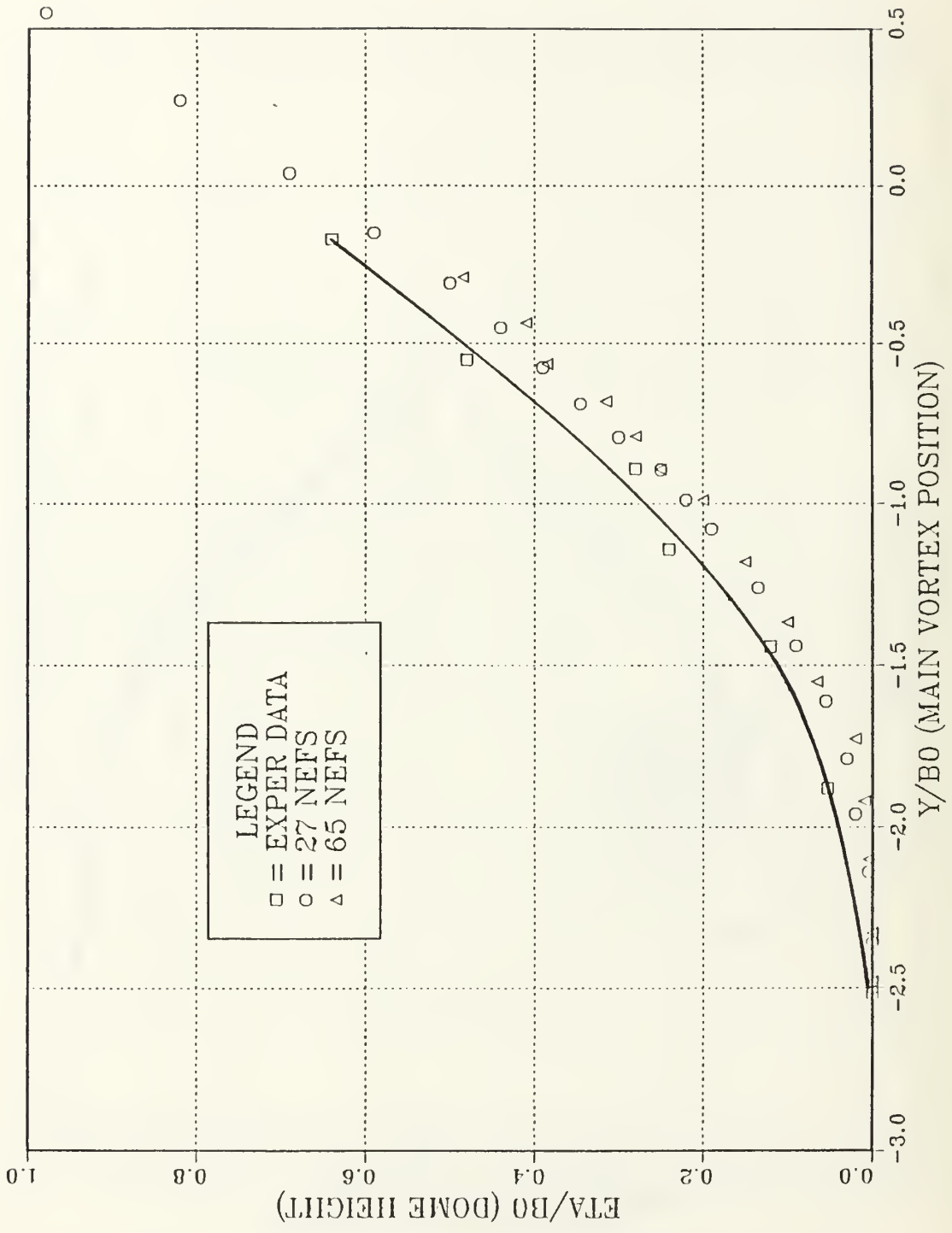

Figure 20. **Comparison of the Measured and Predicted Scar Elevations for Fr = 0.53**

a well-known fact that an infinitesimal disturbance of wavelength λ on a plane sheet of strength γ grows like $\exp(\pi\gamma t/\lambda)$, according to which the shorter waves grow faster [Refs. 18, 23–25]. Clearly, the larger the number of vortices, the smaller the wave length and the faster and sooner the inception of instability, as demonstrated once again by the present calculations. As noted earlier, the instability could have been further delayed by filtering the numerical errors leading to the saw-tooth instability. In fact, this could have yielded scar elevations even larger than those observed experimentally. But the use of an artificial filter has been disregarded. The purpose of the present calculations was not the exact prediction of the ultimate scar shape but rather a search for new insights and inspiration in the simulation of a complex three-dimensional free-surface flow. The challenge was to predict the rate of growth in the face of ever-accumulating errors within a time scale appropriate for the investigation. The numerical model cannot and is not expected to deal with three-dimensional instabilities and turbulence seen during the actual experiments. Although the model has the capability to vary the vortex strength with time to account for the effects of laminar and turbulent diffusion, this was not done. By letting the vortex strength diminish with time, the program may have run longer and the actual height of the humped region may have agreed more closely with the heights seen during the experiments.

IV. CONCLUSIONS

The investigation reported herein warranted the following conclusions:

1. The numerical model, based on the use of a vortex sheet, rediscretization of the sheet segments, and the desingularization of the complex velocity, without the use of an additional numerical filter, is capable of predicting the rate of growth of the free-surface shapes and the location of the early stages of the free surface deformations. The ultimate heights of the scars and striations are dictated by laminar and turbulent diffusion of vortices, surface impurities, and, to a lesser extent, by the initial shape of the counter-rotating vortex pair. The calculations are generally terminated when the free surface forms a sharp corner or when difficulties are encountered in obtaining rapid convergence. There does not seem to be any direct relation between the conditions prevailing at the time of breakdown of the numerical model and the physical conditions existing at the time of attainment of maximum free-surface deformation. Clearly, there are other phenomena, such as turbulence and three-dimensional effects, with which the present numerical model cannot deal.

2. For any of the Froude numbers encountered in the analysis or experiments, no wave train was observed on either side of the scars. This conclusion was somewhat anticipated on the basis of previous calculations. For very small Froude numbers (say, $Fr < 0.15$), the scars were very small, the vortices followed the rigid-wall path, and the scars were slaved to the vortices.

3. Preliminary experiments have revealed the existence of striations even in an otherwise two-dimensional vortex flow. In other words, the striations observed in earlier investigations at the Naval Postgraduate School with an inclined trailing vortex pair [Ref. 26] were not due to the three-dimensionality of the flow. It appears that the striations are a consequence of gravitational and centrifugal instability, in both two- and three-dimensional vortical flows occurring in the vicinity of a free surface. It also appears that the turbulent wake-like features observed in SAR pictures are related to a vortex mechanism: formation of scars and striations, intersection of the striation waves with the edges of the

scars, and the formation of small-scale vortical patterns. These features will be the subject of continuing investigation.

LIST OF REFERENCES

1. Sarpkaya, T., "Trailing-Vortex Wakes on the Free Surface," *Proceedings of the 16th Symposium on Naval Hydrodynamics*, pp. 38–50, National Academy Press, 1986.

2. Naval Postgraduate School Technical Report NPS-69-84-004, *Surface Disturbances Due to Trailing Vortices*, by T. Sarpkaya, and D. O. Henderson, 1984.

3. Tombach, I. H., "Transport of a Vortex Wake in a Stably Stratified Atmosphere," *Aircraft Wake Turbulence and Its Detection*, (ed. J. H. Olsen, et al.), pp. 41–57, Plenum Press, 1971.

4. Barker, S. J., and Crow, S. C., "The Motion of a Two-Dimensional Vortex Pair in Ground Effect," *J. Fluid Mech.*, v. 82, pp. 659-671, 1977.

5. Peace, A. J., and Riley, N., "A Viscous Vortex Pair in Ground Effect," *J. Fluid Mech.*, v. 129, pp. 409–426, 1983.

6. Salvesen, N., and von Kerczek, C., "Comparison of Numerical and Perturbation Solutions of Two-Dimensional Nonlinear Water-Wave Problems," *J. Ship Res.*, v. 20, pp. 160–170, 1976.

7. Lamb, H. (Sir), *Hydrodynamics*, 6th ed., pp. 221–224, Dover Publications, 1945.

8. Sarpkaya, T.; Elnitsky, J.; and Leeker, R. E., "Wake of a Vortex Pair on the Free Surface," *Proceedings of the 17th Symposium on Naval Hydrodynamics*, v. 1, pp. 47–54, 1988 (held at Hague, The Netherlands).

9. Willmarth, W. W.; Tryggvason, G.; Hirsa, A.; and Yu, D., "Vortex Pair Generation and Interaction with a Free Surface" (to appear in *Physics of Fluids*).

10. The University of Michigan Report No. MSM-8707646-88-01, "Dynamics of Vortex Interaction with a Density Interface," by W. J. A. Dahm, C. M. Scheil, and G. Tryggvason, G.

11. Marcus, D. L., *The Interaction Between a Pair of Counter-Rotating Vortices and a Free Boundary*, Ph.D. Thesis, University of California, Berkeley, California, 1988.

12. Telste, J. G., "Potential Flow about Two Counter-Rotating Vortices Approaching a Free Surface," *Journal of Fluid Mechanics*, v. 201, pp. 259–278, 1989.

13. Baker, G. R.; Meiron, D. I.; and Orszag, S. A., "Generalized Vortex Methods for Free-Surface Flow Problems," *J. Fluid Mech.*, v. 123, pp. 477–501, 1982.

14. Zaroodny, S. J., and Greenberg, M. D., "On a Vortex Sheet Approach to the Numerical Calculation of Water Waves," *J. Computational Physics*," v. 11, pp. 440-456, 1973.

15. Kochin, N. E.; Kibel, I. A.; and Roze, N., *Theoretical Hydrodynamics*, Interscience Publishers, 1964.

16. Yeung, R. W., "Numerical Methods in Free Surface Flows," *Ann. Rev. Fluid Mech.*, v. 14, pp. 395–442, 1982.

17. Longuet-Higgins, M. S., and Cokelet, E. D., "The Deformation of Steep Surface Waves, I. A Numerical Method of Computation," *Proc. Roy. Soc., London*, v. A-350, pp. 1-26, 1976.

18. Sarpkaya, T., "Computational Methods with Vortices— 1988 Freeman Scholar Lecture," *Journal of Fluid Mechanics, Trans. ASME*, v. 111, n. 1, pp. 5–52, March 1989.

19. Rosenhead, L., "The Spread of Vorticity in the Wake Behind a Cylinder," *Proc. Roy. Soc.*, Ser. A., v. 127, pp. 590–612, 1930.

20. Roberts, A. J., "A Stable and Accurate Numerical Method to Calculate the Motion of a Sharp Interface between Fluids," *IMA J. Appl. Maths.*, v. 31, pp. 13–35, 1983.

21. Sarpkaya, T., and Shoaff, R. L., "An Inviscid Model of Two-Dimensional Vortex Shedding for Transient and Asymptotically Steady Separated Flow Over a Cylinder," *AIAA J.*, v. 17, n. 11, pp. 1193–1200, 1979.

22. Leeker, R. E., Jr., "Free Surface Scars Due to a Vortex Pair," M.S. and Engineer Degree Thesis, Naval Postgraduate School, Monterey, California, March 1988.

23. Moore, D. W., "A Numerical Study of the Roll-up of a Finite Vortex Sheet," *J. Fluid Mech.*, v. 63, pp. 225–235, 1974.

24. Moore, D. W., "The Rolling Up of a Semi-Infinite Vortex Sheet," *Proc. Roy. Soc. London*, Ser. A, v. 345, pp. 417–430, 1975.

25. Moore, D. W., "The Stability of an Evolving Two-Dimensional Vortex Sheet," *Mathematika*, v. 23, pp. 35–44, 1976.

26. Sarpkaya, T., "Trailing Vortices in Homogeneous and Density-Stratified Media," *Journal of Fluid Mechanics*, v. 136, pp. 85–109, 1983.

INITIAL DISTRIBUTION LIST

		No. Copies
1.	Defense Technical Information Center Cameron Station Alexandria, VA 22304–6145	2
2.	Library, Code 0142 Naval Postgraduate School Monterey, CA 93943-5002	2
3.	Department Chairman, Code 69 Department of Mechanical Engineering Naval Postgraduate School Monterey, CA 93943-5000	1
4.	Professor T. Sarpkaya, Code 69SL Department of Mechanical Engineering Naval Postgraduate School Monterey, CA 93943-5000	5
5.	CDR Douglas H. Rau 2615 Garfield S.E. Port Orchard, WA 98366	2
6.	Office of Naval Research 800 North Quincy Street Arlington, VA 22217	1
7.	Naval Sea Systems Command PMS 350 Washington, D. C. 20362	1
8.	Defense Advanced Research Projects Agency ATTN: S. Resnick 1400 Wilson Blvd. Arlington, VA 22209	1

Thesis
R2445
c.1

Rau
Free surface scars and striations.